JACS
JOURNAL OF THE AMERICAN CHEMICAL SOCIETY
pubs.acs.org/JACS
Article

Programming the Kinetics of Chemical Communication: Induced Fit vs Conformational Selection

Carl Prévost-Tremblay, Achille Vigneault, Dominic Lauzon,* and Alexis Vallée-Bélisle*

Cite This: https://doi.org/10.1021/jacs.4c08597

ABSTRACT: Life on Earth depends on chemical communication and the ability of biomolecular switches to integrate various chemical signals that trigger their activation or deactivation over time scales ranging from microseconds to days. The ability to similarly program and control the kinetics of artificial switches would greatly assist the design and optimization of future chemical and nanotechnological systems. Two distinct structure-switching mechanisms are typically employed by biomolecular switches: induced fit (IF) and conformational selection (CS). Despite 60 years of experimental and theoretical investigations, the kinetic and evolutive advantages of these two mechanisms remain unclear. Here, we have created a simple modular DNA switch that can operate through both mechanisms and be easily tuned and adapted to characterize its thermodynamic and kinetic parameters. We show that the fastest activation rate of a switch occurs when the ligand is able to bind its inactive conformation (IF). In contrast, we show that when the ligand can only bind the active conformation of the switch (CS), its activation rate can be easily programmed over many orders of magnitude by a simple tuning of its conformational equilibrium. We demonstrate the programming ability of both these mechanisms by designing a drug delivery vessel that can be programmed to release a drug over different time scales (>1000-fold). Overall, these findings provide a programmable strategy to optimize the kinetics of molecular systems and nanomachines while also illustrating how evolution may have taken advantage of IF and CS mechanisms to optimize the kinetics of biomolecular switches.

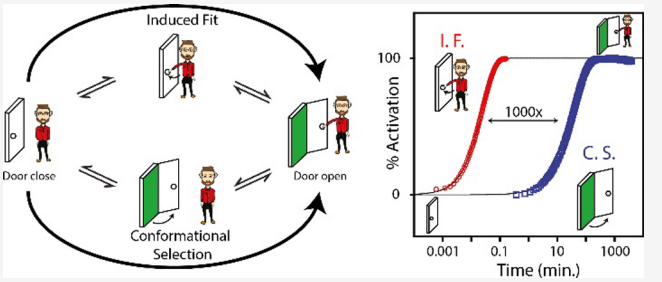

INTRODUCTION

Life is built on biomolecular switches, proteins, or nucleic acids that are activated or deactivated over a wide range of time scales (from milliseconds to months) in response to various stimuli.[1,2] The interaction between biomolecular switches and their ligand is typically achieved through allostery, via two distinct binding-induced conformational change mechanisms: induced fit (IF) and conformational selection (CS).[3,4] These two mechanisms can be easily pictured with the metaphor of an individual opening a door (Figure 1a). In the IF mechanism, the individual grabs the door handle and actively induces its opening (Figure 1a, *top*). In contrast, in the CS mechanism, the individual must wait for the spontaneous opening of the door before grabbing the handle, thus blocking the door into its open conformation (Figure 1a, *bottom*). Similarly, biomolecular switches can also be activated via analogous mechanisms (Figure 1b). More specifically, a switch activated by IF proceeds through ligand binding to the inactive conformation of the switch (bound-inactive), which triggers a structural transition into its bound-active state (Figure 1b, *top*).[5−7] In contrast, a switch activated by CS proceeds through the binding and the stabilization of the active state present among the conformational ensemble of the biomolecular switch (Figure 1b, *bottom*).[5,8,9] Over the last 60 years, both mechanisms have been observed in natural biomolecular switches,[5,10−12] but their advantages and limitations remain unclear.[13−16] While mathematical simulations have suggested that these mechanisms proceed at different rates,[3,4] one main limitation hindering their comprehension is that the natural biomolecular switches that have been characterized so far remain too limited (e.g., different structures, ligands, stabilities, or kinetics). Therefore, they cannot serve as a common ground to identify the structural and thermodynamic determinants of switch performance.[17]

To understand the kinetic and evolutive advantages of the IF and CS mechanisms, here we have engineered a simple artificial biomolecular switch that can be programmed to function via either mechanism. Similar approaches have recently enabled us and others to characterize and better understand the thermodynamic basis of various biochemical mechanisms (e.g., biomolecular switches, homotropic and heterotropic allostery, sequestration mechanism, multivalency, etc.).[18−23] Briefly, this strategy takes advantage of the high simplicity and

Received: July 1, 2024
Revised: October 22, 2024
Accepted: October 23, 2024

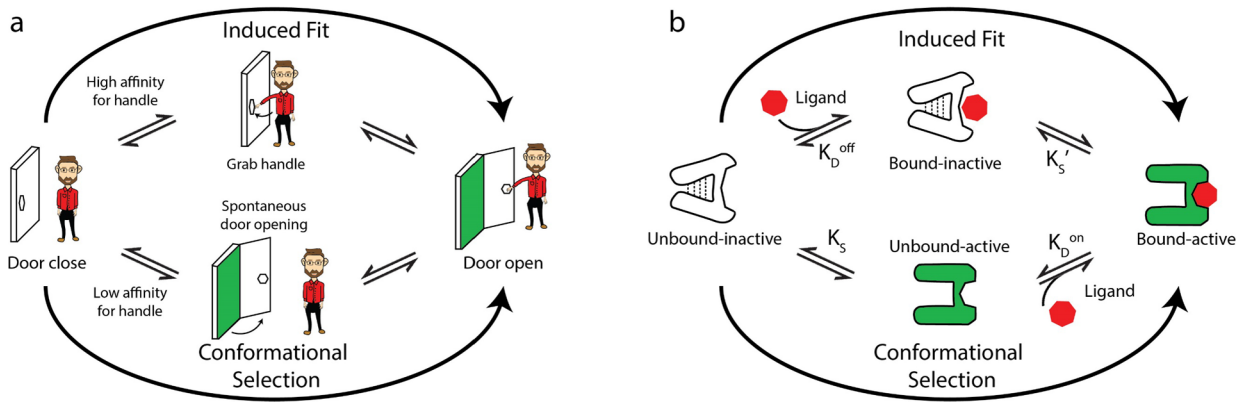

Figure 1. Simple biomolecular switch can function either through an induced fit (IF) or a conformational selection (CS) mechanism. (a) Metaphor of an individual opening a door helps to picture both mechanisms. In the IF mechanism, the individual opens the door by grabbing and pulling its handle. In the CS mechanism, the individual waits for the spontaneous opening of the door and simply keeps it open by grabbing the handle. (b) Four-state thermodynamic cycle of IF and CS mechanisms applied to biomolecular switches. In the IF mechanism, the ligand binds the inactive state of the switch before inducing a conformational change. In the CS mechanism, the ligand only binds and stabilizes the active state present among the conformational ensemble of the biomolecular switch.

programmability of DNA switches, that can be easily designed into various architectures with predictable thermodynamics using simple Watson−Crick base pairs.[24−26] Here, we extend this approach to understand the kinetic determinants of the IF and CS mechanisms to fully exploit their advantages to optimize the design of chemical and nanotechnological systems.

RESULTS

DNA-Based Model. To compare the kinetic performance of CS and IF mechanisms, we have designed a modular DNA switch that can be programmed to activate through either mechanism (Figure 2). The switch adopts a simple bulge duplex conformation in its inactive state and switches into its active conformation upon duplex dissociation. This modular architecture allows for independent tuning, through simple sequence modifications, of three thermodynamic parameters controlling the system (Figure 2a). We can tune the dissociation constant between the ligand and the active conformation, K_D^{on}, by varying the ligand length (red strand). We can tune the conformational equilibrium between the active and inactive conformations, K_S, by varying the hybridization length between the loop (blue) and the reporter (yellow) strands. Most importantly for our analysis, we can also tune the dissociation constant between the ligand and the inactive conformation, K_D^{off}, by varying the loop length (n = number of nucleotides in the loop of the switch). We expect K_D^{off} to be the main determinant of the mechanism since a higher affinity between the inactive state and the ligand (lower K_D^{off}) will favor ligand binding before structure-switching thus favoring the induced fit mechanism (Figure 2a, *bound-inactive intermediate*). Using *mfold*,[27] a nucleic acid secondary structure predictor, we engineered our switches so that the ligand-loop complex (red-blue) displays roughly 1000-fold more affinity than the loop-reporter duplex (blue-yellow) thus ensuring a robust response upon ligand addition (Table S1). Real-time monitoring of the activation/deactivation processes can be readily obtained using a fluorophore and quencher pair located at the opposite ends of either the reporting DNA strand (activation, see Figure 2b) or the ligand (deactivation, see Figure 2c).

Switch Stabilities. To compare the IF and CS mechanisms, we created two switches differing only in their affinities between the ligand and the inactive state of the switch (different K_D^{off}). We did so by designing two switches with similar K_S and K_D^{on} (same 17 nucleotides recognition element) but with different loop lengths (1 and 10 nucleotides) thus providing different levels of accessibility of the recognition element in the inactive state (different K_D^{off}) (Figure S1 and Table S1). A 10-nucleotide loop (low K_D^{off}) should display sufficient affinity to enable ligand binding to the inactive conformation in the nanomolar concentration range (Figure 2a, *top*).[28] In contrast, we expect that the 1 nucleotide loop switch (high K_D^{off}) should display an insufficient affinity for the ligand in its inactive conformation thus requiring switch dissociation before ligand binding (Figure 1a, *bottom*). Using urea denaturation curves,[29] we confirmed that both switches display similar K_S (-13.1 ± 0.4 and -12.2 ± 0.3 kcal mol^{-1} for loop-1 and loop-10 switches, respectively, Figure S1), and similar affinity for their respective ligands (K_D^{on}) (-20.5 ± 0.7 and -20.9 ± 0.7 kcal mol^{-1} for loop-1 and loop-10 switches, respectively, Figure S2). We also confirmed that they display similar rates of opening and closing in the absence of ligand (within 3-fold, see Figure S3 and Table S2), and similar hybridization rates between the ligand and the active state k_{on} (within 3-fold, see Figure S4). In these conditions, any further kinetic variation observed between these switches should be attributable to variation between the ligand and the inactive state affinity (K_D^{off}).

Activation Kinetics. We compared the activation kinetics of both switches by measuring the activation rates in the presence of varying concentrations of ligand (Figure 2b). The kinetic time courses of the loop-1 and loop-10 switches are well fit using a single exponential function (Figure S5). We found that the loop-10 switch (k_{obs} = 40 min^{-1}) is activated roughly 1000-fold faster than the loop-1 switch (k_{obs} = 0.025 min^{-1}) at their highest concentration of ligand (50 μM). The activation rates of both switches increase proportionally with the concentration of ligand (Figure 2b *bottom*). This indicates that ligand binding (and not reporter dissociation) represents the rate-limiting step of the activation mechanism. Therefore, the faster activation of the loop-10 switch likely results from ligand binding to the highly populated, higher affinity inactive state (see bound-inactive state in Figure 2a).

Deactivation Kinetics. According to the detailed balance principle, two switches of similar equilibrium but different activation rates must also deactivate with proportionally

https://doi.org/10.1021/jacs.4c08597
J. Am. Chem. Soc. XXXX, XXX, XXX−XXX

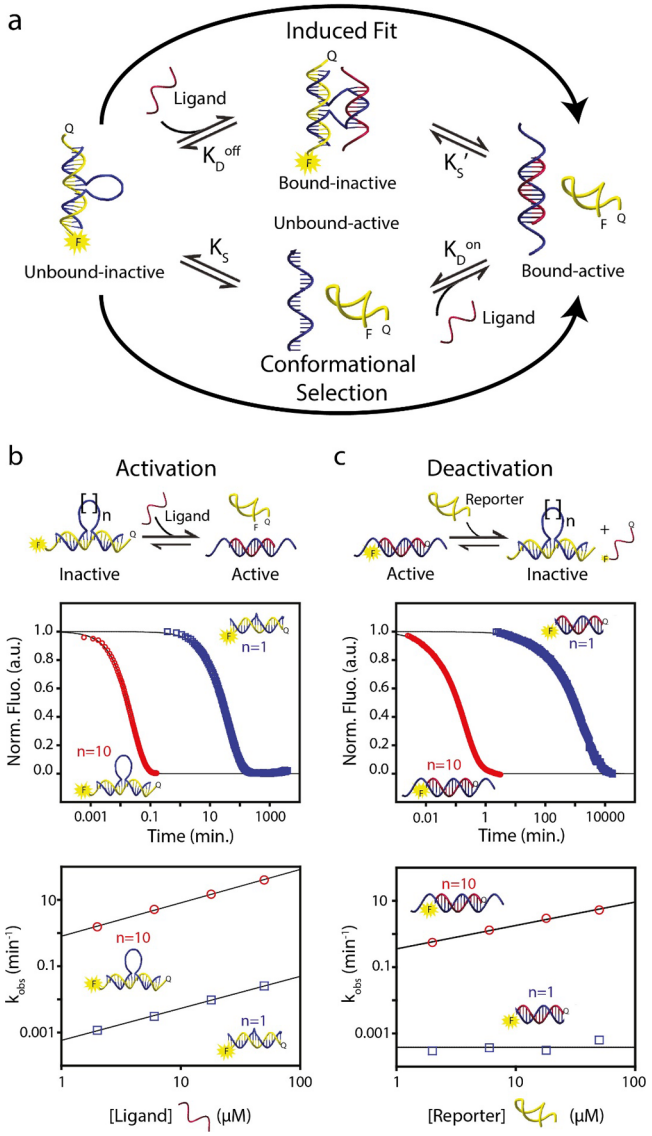

Figure 2. Increasing the accessibility of the binding site in the inactive state (e.g., 10 nucleotides versus 1 nucleotide) accelerates the activation and deactivation rates of the switch. (a) A model DNA switch with tunable thermodynamics. We hypothesize that the level of accessibility of the recognition site (length of the loop: $[\ ]_n$) in the inactive state will determine whether the switch is activated through induced fit (high accessibility) or conformational selection (low accessibility) mechanisms. Fluorophore (F) and quencher (Q) are positioned at locations enabling switch activation monitoring. (b) *Top.* Activation time courses of switches with a loop containing 1 nucleotide (n = 1, *blue*) or 10 nucleotides (n = 10, *red*) in the presence of 50 μM of ligand (perfectly matched 17 nucleotides DNA ligand) fit to a single exponential function (Figure S5). *Bottom.* Observed rates of activation (k_{obs}) of both switches increase with ligand concentration, suggesting that ligand binding is rate-limiting for both switches. (c) *Top.* Deactivation time courses of the different switches (n = 1 and n = 10) in the presence of 50 μM of unlabeled reporter strand fit a stretched exponential function (see Figure S6). *Bottom.* Observed rates of deactivation (k_{obs}) of the loop-10 switch, and not the loop-1 switch, increase with ligand concentration. Each kinetic experiment was performed once (n = 1).

different rates (Figure 2c). The deactivation process can be initiated by adding an excess of unlabeled reporter strand (yellow) to a solution of active complex (i.e., loop hybridize to fluorescently labeled ligand) (see Figure S6). We found that the loop-10 switch (k_{obs} = 5.3 min^{-1}) indeed deactivates roughly 8000-fold faster than the loop-1 switch (k_{obs} = 0.00063 min^{-1}). We also found that the deactivation rate of the loop-1 switch is independent of the reporter strand concentration, indicating that ligand dissociation is rate-limiting. In contrast, the deactivation rate of loop-10 switch is proportional to the reporter concentration (Figure 2c, *bottom*). This indicates that the reporter binding (i.e., the conformational change) is rate limiting and that ligand dissociation is accelerated following reporter binding through the formation of an induced fit intermediate similar to the one suggested by the activation kinetics (see bound-inactive state in Figure 1b).

Effect of K_S on the Activation Kinetics. Distinguishing between IF and CS solely based on concentration-dependent experiments, however, cannot be an unequivocal proof, especially for the IF mechanism.[30] Therefore, to confirm that the large kinetic variation observed between both switches is attributable to the use of distinct intermediate states, we examined how their kinetic is affected by their stability (Figure 3, *top*). To do so, we designed several variants of the loop-1 and loop-10 switches with different conformational equilibriums (K_S) by varying the hybridization length between the reporter and loop strands (see Methods). In the present case, where switch activation is limited by the rate of ligand binding (Figure 2a, *bottom*), the kinetic model of CS (Figure S7) predicts that the rate of this mechanism will decrease proportionally with the active state concentration (Figure S8), i.e., the ligand does not bind the inactive state (Figure S9). Indeed, decreasing K_S reduces the unbound-active state concentration and decreases the CS reaction rate by over 1000-fold, thus supporting the CS mechanism in the case of loop-1 (Figure 3, *top*, *blue*). In contrast, the kinetic model of IF (Figure S7) predicts that the rate of activation is proportional to the inactive state concentration, which remains relatively independent of K_S in the useful switching range (Figure S9). Indeed, we observe that the activation rate of the loop-10 switch is independent of K_S, and thus independent of the [unbound-active], confirming that ligand binding does not occur on the active state but rather binds the inactive conformation, thus supporting the IF mechanism (Figure 3, *top*, *red*). As anticipated, the activation rate of both mechanisms converges at a higher K_S value where a significant fraction of the switch is already in the active conformation (~20%) in the absence of ligands (Figure S8).

We have also designed and measured the activation kinetics of three other switches (loop-4, loop-7, and loop-13), displaying different loop lengths (Figure S11). As expected, the smaller loop-4 proceeds via a CS mechanism like loop-1, with its activation kinetics being dependent on K_S. In contrast, the longer loop-7 and loop-13 activation kinetics were found independent of K_S, suggesting that they proceed via an IF mechanism like loop-10. Of note, the transition between a CS mechanism (short loop) and an IF mechanism (long loop) happens close to seven nucleotides, reminiscent of the "*rule of seven*" in base pairing.[28] Overall, all these activation kinetics results demonstrate that the IF mechanism enables fast ligand-responsive switches, even for highly stable switches that display low background activity. They also highlight that the activation rates of CS switches can be easily programmed over more than 3 orders of magnitude (>1000x) by simply varying their stability (K_S).

Effect of K_S on the Deactivation Kinetics. To confirm that the deactivation proceeds through the same mechanism and thus through the same intermediate state as in the activation, we

https://doi.org/10.1021/jacs.4c08597
J. Am. Chem. Soc. XXXX, XXX, XXX−XXX

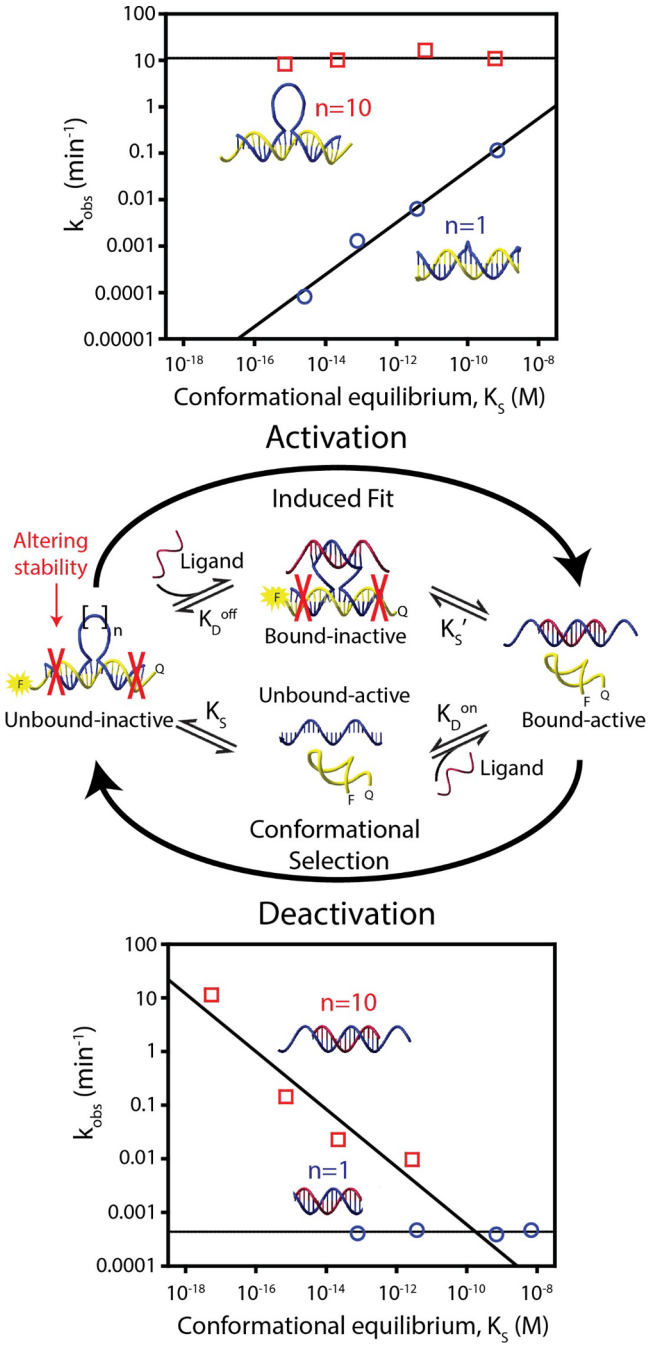

Figure 3. Increasing the stability of the inactive state decreases the activation rate of the CS mechanism and increases the deactivation rate of the IF mechanism. *Top.* Activation rate (k_{obs}) of the loop-1 switch (n = 1, *blue*) increases linearly as the inactive state is destabilized. In contrast, the activation rate of the loop-10 switch (n = 10, red) remains independent of the switching equilibrium (K_S). See Figure S10 for the kinetic traces. *Bottom.* Deactivation rate (k_{obs}) of the loop-10 switch (n = 10, *red*) decreases linearly as the inactive state is destabilized. In contrast, the deactivation rate of the loop-1 switch (n = 1, *blue*) remains independent of the switching equilibrium (K_S). See Figure S13 for the kinetic traces. Activation experiments were performed in the presence of 10 μM of ligand while deactivation experiments were performed in the presence of 10 μM of unlabeled reporter strand. Each kinetic experiment was performed once (n = 1).

also analyzed the effect of varying the conformational equilibrium (K_S) on the deactivation rates (Figure 3, *bottom*). The kinetic model of CS (Figure S7) predicts that the deactivation rate of this mechanism will remain unaffected by the conformational equilibrium since the deactivation is limited by ligand dissociation (Figure S12). Indeed, we observe that stabilizing the reporter-loop duplex (i.e., the inactive state) does not affect the deactivation rate of the loop-1 switch (k_{obs} = 0.0043 ± 0.004 min^{-1}) (Figure 3, top, red). In contrast, the kinetic model of IF (Figure S7) predicts that the deactivation is triggered by the association of the reporter strand. The deactivation rate therefore increases when stabilizing the conformational equilibrium (K_S). As expected, we observe that stabilizing the reporter-loop duplex (i.e., the inactive state) increases the deactivation rate by 1000-fold when varying K_S by a similar extent (Figure 3, *bottom, red*). This confirms that the added/removed base pairs in the loop-10 switch become hybridized in the bound-inactive intermediate, which lowers the deactivation energy barrier (i.e., these added/removed base pairs are not present in the bound-active conformation). Furthermore, by analyzing the effect of mutating the tails of the loop-10 switch (Figure S14), we confirmed that both tails of the switch are hybridized in the inactive-bound intermediate. These results also suggest that the activation and deactivation of the IF switch proceeds through the same inactive-bound intermediate conformation.

Mechanism Principles. Overall, these results demonstrate that the fast activation and deactivation rates of the IF mechanism (loop-10) is attributable to the presence of a relatively stable bound-inactive transition state (Figure 4). By stabilizing the inactive state (K_S), the bound-inactive transition state is stabilized to the same extent (black arrows). Therefore, the activation rate of an IF switch cannot be programmed to be faster or slower since the activation energy (E_A) remains the same. However, since the deactivation proceeds from the active state, the lower energy barrier of the bound-inactive transition state provided by a stabilization of K_S enables to accelerate its deactivation. In contrast, in the CS mechanism (loop-1), the switch cannot have access to the inactive-bound transition state because this latter is too unstable (not enough nucleotides available in the loop to interact with the ligand strand). Therefore, the deactivation remains relatively slow and cannot be programmed by tuning the stability of the inactive state (K_S). However, its activation rate can be slowed down (or accelerated) by stabilizing (or destabilizing) the inactive state.

Kinetically Programmed Drug Delivery Nanomachines. In this study, the DNA-based loop-reporter switch served as a simple, programmable system to understand the kinetic and evolutive advantages of the IF and CS mechanisms. To enable a stringent test of our understanding of these mechanisms, we have designed a nanomachine that can be programmed to deliver drugs at a specific time scale (Figure 5). This nanomachine contains two modules. The first "timer" module consists of the same loop-reporter switch that enables the precise programming of the release rate of a reporter strand (Figure 5a, *left*). This reporter strand then activates a drug-transporting module that enables the release of a specific drug (quinine) (Figure 5a *right*). Briefly, we have designed the reporter strand to be fully complementary to a drug-binding aptamer (i.e., quinine aptamer) (see Figure S15 for aptamer design).[31] A 10-time excess of ligands is used to activate the loop-reporter complex, ensuring the reporter strand does not bind back to the loop and specifically hybridizes with the aptamer, thus releasing the quinine. Conveniently, the release of quinine can be directly monitored by an increase in its

https://doi.org/10.1021/jacs.4c08597
J. Am. Chem. Soc. XXXX, XXX, XXX−XXX

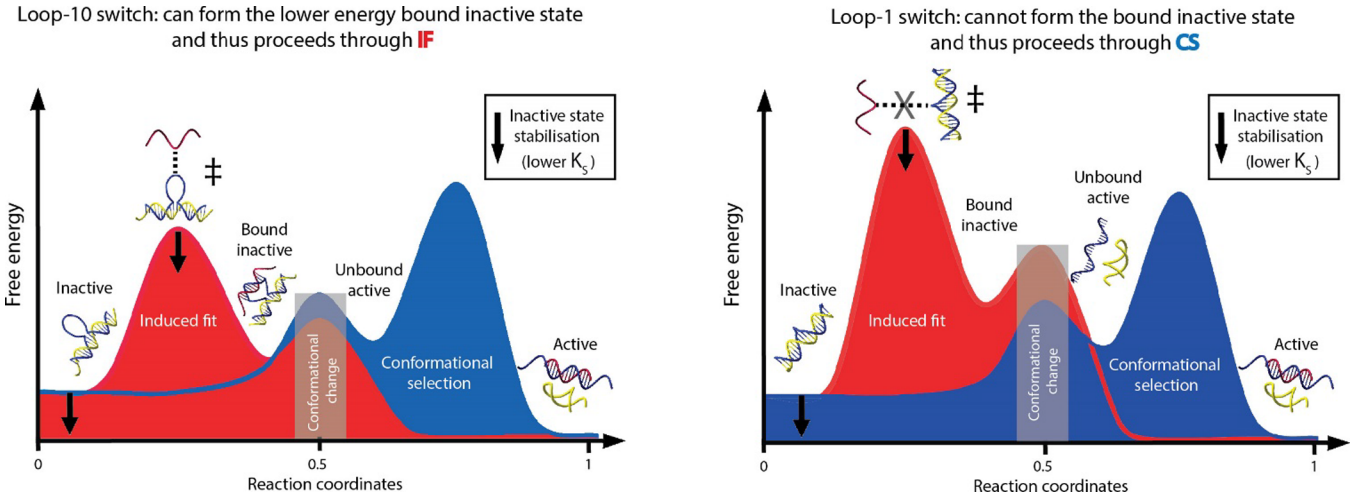

Figure 4. Induced fit accelerates the activation and deactivation rates of biomolecular switches by creating a lower energy path via a bound-inactive transition state. Energy diagrams of both conformational selection (blue) and induced fit (red) mechanisms illustrate the effect of stabilizing the inactive state.

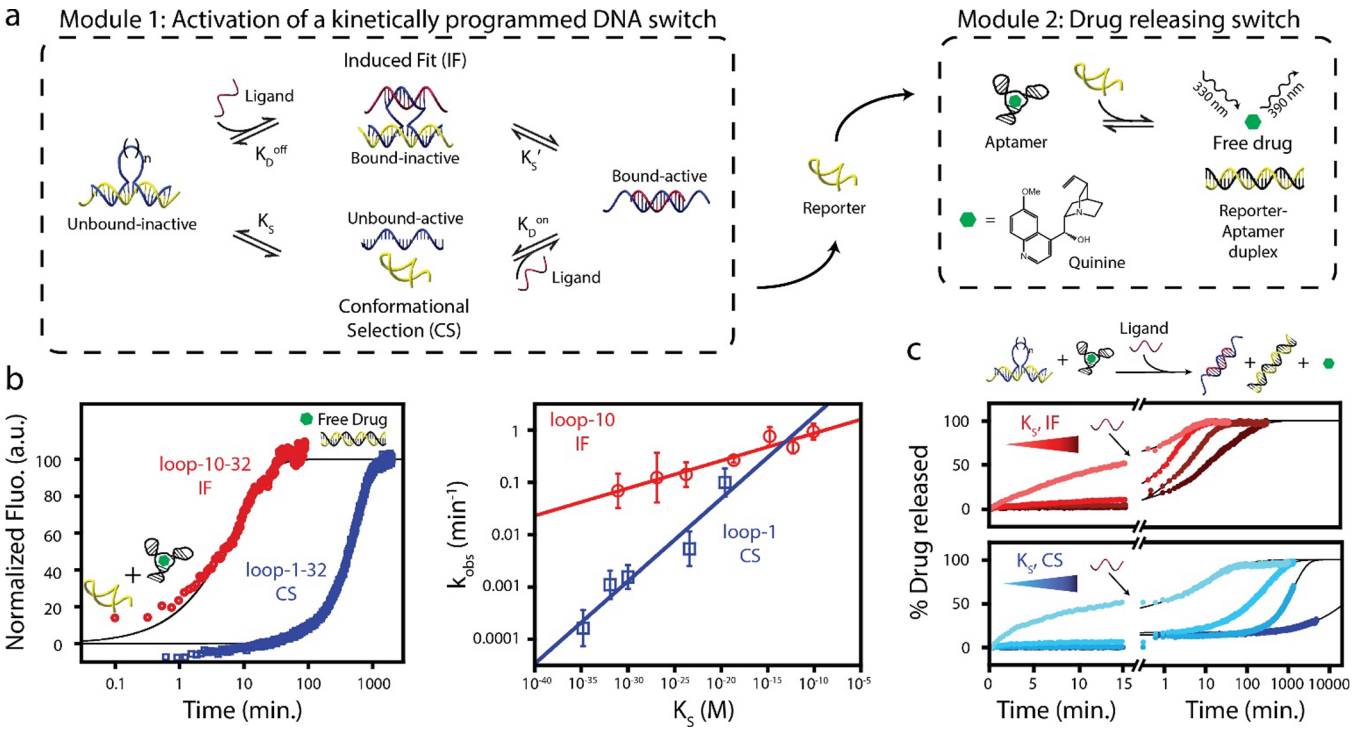

Figure 5. Kinetically programmed induced fit (IF) or conformational selection (CS) drug-releasing nanomachines. (a) Drug-releasing nanomachine is composed of two modules: 1) a DNA switch with programmable kinetic (IF or CS) and 2) an aptamer-based drug-releasing switch. Reporter (yellow) is first sequestered by the loop (blue) and its release is kinetically triggered by the addition of a ligand (red) via either IF or CS mechanisms. When freed, the reporter can hybridize with the aptamer (black) and release the drug (green, quinine). Liberation of quinine is followed by an increase in fluorescence. (b) *Left*. IF (loop-10−32, red) allows for a faster release of drugs compared to the CS mechanism (i.e., 30-fold) with switches of similar stabilities (K_S, Tables S7 and S8). *Right*. As expected, the rate of drug release can be easily programmed by tuning of K_S of the CS switch, while the rate of an IF switch remains relatively constant over different K_S (Figure S19). Error bars represent the standard deviation of three replicates ($n = 3$). (c) While a stable IF switch allows for rapid drug release without drug leakage (red), CS switches allow the precise tuning of the drug release rate over 1000-fold variation by simply tuning their K_s (blue). Of note, for an easy comparison of the time scale difference between IF and CS, the *x*-axis scaling changes from linear to logarithmic after the addition of the ligand (see Figure S20 for a linear representation).

fluorescence (see Figure S16 for the fluorescent monitoring workflow).[32]

We first designed an IF and a CS drug-releasing nanomachines exhibiting similar conformational equilibrium. More specifically, we started by selecting a quinine aptamer displaying stability that offers an ideal trade-off between high drug affinity and rapid hybridization rate with its fully complementary sequence, the reporter strand (aptamer 32 nt, Figure S15).[31] We then designed the IF loop with tails that are fully complementary to this reporter strand (loop-10−32) and measured its conformational equilibrium ($K_{S,IF} = 8 \times 10^{-32}$, Figure S17). Finally, we designed a ligand strand that can hybridize with the

https://doi.org/10.1021/jacs.4c08597
J. Am. Chem. Soc. XXXX, XXX, XXX−XXX

exposed loop with a sufficient affinity to displace the reporter strand (a perfectly matched 22 nucleotide sequence, see Tables S7 and S8). Of note, we designed a different reporter strand for the CS system to avoid significant interaction between the ligand and the aptamer due to their high sequence complementarity (loop-1−32, see SI for more details). We found that a DNA reporter containing two perfectly complementary 16-nucleotide tails separated by a one-nucleotide loop displays a similar conformational equilibrium than the loop-10−32 switch ($K_{S,CS} = 1 \times 10^{-32}$, Figure S18). As expected from switches with similar conformational equilibrium (K_S), we found that the IF switch allows for a much faster drug release rate compared to the CS switch (i.e., 30-fold, Figure 5b, *left*).

We then took advantage of the programming ability of these two switching mechanisms to design nanomachines with different drug-releasing rates (Figure S19). As expected, when employing nanomachines activated through IF (i.e., loop-10), stabilizing the unbound-inactive conformation by over 12.2 kcal/mol^{-1} had only a small effect on the release rate of quinine (i.e., less than 10-fold variation). In contrast, stabilizing the unbound-inactive conformation of the nanomachine activated by CS (i.e., loop-1) by up to 8.9 kcal/mol^{-1} allows to decrease the kinetic of drug release by over 1000-fold (Figure 5b, *right*).

An important consideration in the design of these two mechanisms is also the impact that the conformation equilibrium (K_S) has on the basal activity of the nanomachine. For example, we found that IF and CS nanomachines with low conformational equilibrium ($K_S > 10^{-20}$ M) also display significant drug leakage as shown by the increase of fluorescence in the absence of ligand (see light red and light blue curves Figure 5c). This is due to the low affinity of the loop-reporter duplex, which allows for the spontaneous dissociation of the reporter strand. Therefore, since the aptamer and the loop are competing for the reporter, the aptamer can hybridize the reporter and release the drug. One obvious advantage of the IF nanomachine over a CS nanomachine is that the loop-reporter complex can be further stabilized to reduce aptamer competition for the reporter, and that, without reducing the kinetic of drug release (Figure 5c). In contrast, since the rate of a CS switch relies on the concentration of the unbound-active state, faster CS switches will always result in higher drug leakage (i.e., low drug leakage leads to slower drug release). Overall, these experiments exemplify how we can take advantage of the IF and CS mechanisms to program the activity of nanomachines.

DISCUSSION

To expand our understanding of the kinetic programming at the basis of chemical communication, here, we compared the kinetic performance of two binding-induced conformational change mechanisms, IF and CS, on similar DNA biomolecular switches. Based on previous theoretical studies,[3,4] we hypothesized that the key design feature differentiating those mechanisms resides in the accessibility of their binding sites in their inactive state, quantified by K_D^{off}. We found that the switch with the least accessible binding site (loop-1: only one nucleotide available for binding in the inactive state) requires switching (dissociation) into its highly accessible active state before ligand binding, thus operating through a CS mechanism. Using the door analogy, this mechanism requires spontaneous opening of the door before the individual/target can bind and block the door into its open conformation. Upon increasing the accessibility of the binding site using a loop of 10 nucleotides, we found that the favored path to ligand binding now proceeds via the formation of a three-strand induced fit intermediate, which accelerates the activation of the switch by up to 1000-folds. Using the door analogy, this mechanism implies that the individual/target grabs the handle and actively induces the opening of the door, thus resulting in faster activation. Following the principle of detailed balance, we also found that the deactivation of the loop-10 switch is also 800-fold faster than the corresponding loop-1 switch. Investigation of the mechanism underlying this kinetic difference revealed that loop-10 switch is also deactivated via an induced fit mechanism while loop-1 switch still employs a conformational selection mechanism. This kinetic difference can be explained by the fact that conformational switching to the bound inactive state allows the ligand to dissociate faster from the lower affinity inactive state of loop-10 by induced fit (Figure 4, *left*). In contrast, the dissociation of the ligand from the higher affinity active state of loop-1 resulted in a slower deactivation through conformational selection (Figure 4, *right*). Overall, increasing the accessibility of the binding site in the inactive state (K_D^{off}) increases the kinetics of its binding-induced activation via a change of mechanism (CS to IF).

Other approaches for programming the activation/deactivation rates of biomolecular switches exist. One involves kinetic traps to program the activation of DNA-based assembly or protein complexes.[23] However, kinetic trapping, as the name implies, is not a viable method for accelerating activation. Instead, it serves to postpone the activation until a later point in time. Acceleration could instead be achieved by using a programmable toehold domain that promotes strand displacement reaction and, thus, switch activation.[33,34] However, this strategy is limited to DNA-based nanosystems, while IF and CS are protein-inspired strategies that could potentially be implemented into the design of *de novo* protein switches. Finally, multivalency is another mechanism that differs from the ligand-induced allosteric mechanism presented herein.[22] While this strategy is easier to implement design-wise compared to these allosteric strategies, it only allows for the programming of the deactivation kinetics of molecular switches. Thus, in addition to the strategies mentioned above, CS and IF offer a complementary design strategy to program either the activation or deactivation rate of biomolecular switches by carefully designing the accessibility of the ligand binding domain.

These findings also have wide implications for our ability to rationally tune the kinetics of therapeutic molecules and man-made nanomachines. The residence time of a drug, for example, is an important parameter in the development of efficient therapeutic molecules.[35] However, the rational optimization of residence times remains tedious due to the lack of understanding of the "structure-kinetic relationships".[36] Considering that the efficiency of drugs is typically enhanced by slower dissociation rates,[35,36] our results, therefore, suggest that compounds designed to interact with their protein target via a conformational selection mechanism should see their activity enhanced. On the other hand, compounds targeting selectively the inactive state are also susceptible to genetic or adaptive mechanisms of resistance.[37,38] For instance, selective inhibitors that target the inactive state of RAS-GTPase are susceptible to perturbations that drive the equilibrium toward the active state.[39] In such cases, compounds that target and inhibit the active state could be developed to counteract this issue. For example, ON-state KRAS inhibitors were recently developed that display faster inactivation rates, while OFF-state selective inhibitors are often found to be rate-limited by GTP hydrolysis (i.e., switching into the GDP-bound inactive state).[38,40]

https://doi.org/10.1021/jacs.4c08597
J. Am. Chem. Soc. XXXX, XXX, XXX−XXX

We also believe that artificial nanomachines used for drug delivery could benefit from a better understanding of the IF and CF mechanisms. Using quinine and its aptamer as a model drug delivery vessel (Figure 5),[31] we showed that the IF mechanism, for example, could be employed to design artificial nanomachines that allow for a fast release of drug with minimized drug leakages. In contrast, the CS mechanism allows for a slower ligand-mediated release of a molecular cargo which could help maintain the concentration of drugs under the therapeutic window over an extended period.[41,42] We believe that the next generation of drug delivery systems could benefit from the slower kinetics properties provided by a CS mechanism or from the fast, immediate-release kinetics properties provided by an IF mechanism.

Overall, the distinct evolutionary roles and advantages of these two signaling mechanisms begin to emerge. Biomolecules involved in processes requiring rapid equilibration (e.g., proteins involved in sensing processes or that trigger rapid movement or responses) would benefit from the induced fit kinetic properties. In contrast, some processes must operate on slower time scales, like the inhibition of certain proteases which can last up to three months.[43] In such cases, the conformational selection mechanism could have been evolutionarily favored to allow regulation on such a slow time scale. In addition, single point mutations that stabilize or destabilize the conformational equilibrium (K_S) of a biomolecular switch could have also served as a path to evolve the deactivation rate or the activation rate of biomolecular switches under the IF or CS mechanisms, respectively. For example, studies on protein[44] and DNA-based[45,46] switches have demonstrated how the rate of ligand binding could be optimized through simple mutagenesis analysis. In perspective, we believe that a better understanding of the IF and CS mechanisms can provide protein engineers and nanoengineers with a kinetic framework to create responsive nanosystems with highly controlled kinetics, while also providing new insights to better understand the evolution of biomolecular systems.

■ ASSOCIATED CONTENT

Supporting Information

The Supporting Information is available free of charge at https://pubs.acs.org/doi/10.1021/jacs.4c08597.

Materials and methods, DNA sequences, supporting figures and supporting tables, raw data, and fitting equations (PDF)

■ AUTHOR INFORMATION

Corresponding Authors

Dominic Lauzon − *Département de Chimie, Laboratoire de Biosenseurs et Nanomachines, Université de Montréal, Montréal, QC H2V 0B3, Canada;* orcid.org/0000-0002-7513-3233; Email: dominic.lauzon@umontreal.ca

Alexis Vallée-Bélisle − *Département de Biochimie et Médecine Moléculaire, Institut de Génie Biomédical, Département de Pharmacologie et Physiologie, and Département de Chimie, Laboratoire de Biosenseurs et Nanomachines, Université de Montréal, Montréal, QC H2V 0B3, Canada;* orcid.org/0000-0002-5009-7715; Email: a.vallee-belisle@umontreal.ca

Authors

Carl Prévost-Tremblay − *Département de Biochimie et Médecine Moléculaire, Université de Montréal, Montréal, QC H2V 0B3, Canada*

Achille Vigneault − *Institut de Génie Biomédical, Département de Pharmacologie et Physiologie, Université de Montréal, Montréal, QC H2V 0B3, Canada*

Complete contact information is available at: https://pubs.acs.org/10.1021/jacs.4c08597

Author Contributions

The manuscript was written through contributions of all authors. All authors have given approval to the final version of the manuscript.

Notes

The authors declare no competing financial interest.

■ ACKNOWLEDGMENTS

A.V.-B. acknowledges the Natural Sciences and Engineering Research Council of Canada (Conseil de Recherches en Sciences Naturelles et en Génie du Canada) − RGPIN-2020-06975 − for funding this work. A.V.-B. is Canada Research Chair in Bioengineering and Bionanotechnology, Tier II. C.P.-T. acknowledges the Natural Sciences and Engineering Research Council of Canada for a doctoral scholarship. A.V. acknowledges a scholarship from PROTEO.

■ ABBREVIATIONS

K_S, switching equilibrium constant; K_D^{off}, dissociation constant between the ligand and the *inactive* conformation; K_D^{on}, dissociation constant between the ligand and the *active* conformation; k_{on}, association rate constant; k_{off}, dissociation rate constant; k_{obs}, observed rate constant; nt, nucleotide

■ REFERENCES

(1) Alon, U. Simplicity in biology. *Nature* **2007**, *446* (7135), 497−497.

(2) Alon, U. *An introduction to systems biology: design principles of biological circuits*; Chapman and Hall/CRC: 2006.

(3) Weikl, T. R.; von Deuster, C. Selected-fit versus induced-fit protein binding: Kinetic differences and mutational analysis. *Proteins: Struct., Funct., Bioinf.* **2009**, *75* (1), 104−110.

(4) Kiefhaber, T.; Bachmann, A.; Jensen, K. S. Dynamics and mechanisms of coupled protein folding and binding reactions. *Curr. Opin. Struct. Biol.* **2012**, *22* (1), 21−29.

(5) Boehr, D. D.; Nussinov, R.; Wright, P. E. The role of dynamic conformational ensembles in biomolecular recognition. *Nat. Chem. Biol.* **2009**, *5* (11), 789−796.

(6) Koshland, D. E. Application of a Theory of Enzyme Specificity to Protein Synthesis. *Proc. Natl. Acad. Sci. U. S. A.* **1958**, *44* (2), 98−104.

(7) Segel, I. H. *Enzyme kinetics: behavior and analysis of rapid equilibrium and steady state enzyme systems*; John Wiley & Sons: 1975.

(8) Monod, J.; Wyman, J.; Changeux, J.-P. On the nature of allosteric transitions: A plausible model. *J. Mol. Biol.* **1965**, *12* (1), 88−118.

(9) Tsai, C.-J.; Kumar, S.; Ma, B.; Nussinov, R. Folding funnels, binding funnels, and protein function. *Protein Sci.* **1999**, *8* (6), 1181−1190.

(10) Wright, P. E.; Dyson, H. J. Linking folding and binding. *Curr. Opin. Struct. Biol.* **2009**, *19* (1), 31−38.

(11) Copeland, R. A. Conformational adaptation in drug−target interactions and residence time. *Future Med. Chem.* **2011**, *3* (12), 1491−1501.

(12) Daniels, K. G.; Tonthat, N. K.; McClure, D. R.; Chang, Y.-C.; Liu, X.; Schumacher, M. A.; Fierke, C. A.; Schmidler, S. C.; Oas, T. G.

Ligand Concentration Regulates the Pathways of Coupled Protein Folding and Binding. *J. Am. Chem. Soc.* **2014**, *136* (3), 822−825.
(13) Daniels Kyle, G.; Suo, Y.; Oas, T. G. Conformational kinetics reveals affinities of protein conformational states. *Proc. Natl. Acad. Sci. U. S. A.* **2015**, *112* (30), 9352−9357.
(14) Hammes Gordon, G.; Chang, Y.-C.; Oas, T. G. Conformational selection or induced fit: A flux description of reaction mechanism. *Proc. Natl. Acad. Sci. U. S. A.* **2009**, *106* (33), 13737−13741.
(15) Greives, N.; Zhou, H.-X. Both protein dynamics and ligand concentration can shift the binding mechanism between conformational selection and induced fit. *Proc. Natl. Acad. Sci. U. S. A.* **2014**, *111* (28), 10197−10202.
(16) Gianni, S.; Dogan, J.; Jemth, P. Distinguishing induced fit from conformational selection. *Biophys. Chem.* **2014**, *189*, 33−39.
(17) Tokuriki, N.; Tawfik, D. S. Stability effects of mutations and protein evolvability. *Curr. Opin. Struct. Biol.* **2009**, *19* (5), 596−604.
(18) Vallée-Bélisle, A.; Ricci, F.; Plaxco, K. W. Thermodynamic basis for the optimization of binding-induced biomolecular switches and structure-switching biosensors. *Proc. Natl. Acad. Sci. U. S. A.* **2009**, *106* (33), 13802−13807.
(19) Simon, A. J.; Vallée-Bélisle, A.; Ricci, F.; Watkins, H. M.; Plaxco, K. W. Using the Population-Shift Mechanism to Rationally Introduce "Hill-type" Cooperativity into a Normally Non-Cooperative Receptor. *Angew. Chem., Int. Ed.* **2014**, *53* (36), 9471−9475.
(20) Ricci, F.; Vallée-Bélisle, A.; Porchetta, A.; Plaxco, K. W. Rational Design of Allosteric Inhibitors and Activators Using the Population-Shift Model: In Vitro Validation and Application to an Artificial Biosensor. *J. Am. Chem. Soc.* **2012**, *134* (37), 15177−15180.
(21) Ha, S. H.; Ferrell, J. E. Thresholds and ultrasensitivity from negative cooperativity. *Science* **2016**, *352* (6288), 990−993.
(22) Lauzon, D.; Vallée-Bélisle, A. Programing Chemical Communication: Allostery vs Multivalent Mechanism. *J. Am. Chem. Soc.* **2023**, *145* (34), 18846−18854.
(23) Lauzon, D.; Vallée-Bélisle, A. Functional advantages of building nanosystems using multiple molecular components. *Nat. Chem.* **2023**, *15* (4), 458−467.
(24) Harroun, S. G.; Prévost-Tremblay, C.; Lauzon, D.; Desrosiers, A.; Wang, X.; Pedro, L.; Vallée-Bélisle, A. Programmable DNA switches and their applications. *Nanoscale* **2018**, *10* (10), 4607−4641.
(25) Seeman, N. C.; Sleiman, H. F. DNA nanotechnology. *Nat. Rev. Mater.* **2018**, *3* (1), 17068.
(26) Wang, F.; Liu, X.; Willner, I. DNA Switches: From Principles to Applications. *Angew. Chem., Int. Ed.* **2015**, *54* (4), 1098−1129.
(27) Zuker, M. Mfold web server for nucleic acid folding and hybridization prediction. *Nucleic Acids Res.* **2003**, *31* (13), 3406−3415.
(28) Cisse, I. I.; Kim, H.; Ha, T. A rule of seven in Watson-Crick base-pairing of mismatched sequences. *Nat. Struct. Mol. Biol.* **2012**, *19* (6), 623−627.
(29) Idili, A.; Ricci, F.; Vallée-Bélisle, A. Determining the folding and binding free energy of DNA-based nanodevices and nanoswitches using urea titration curves. *Nucleic Acids Res.* **2017**, *45* (13), 7571−7580.
(30) Chakraborty, P.; Di Cera, E. Induced Fit Is a Special Case of Conformational Selection. *Biochemistry* **2017**, *56* (22), 2853−2859.
(31) Reinstein, O.; Yoo, M.; Han, C.; Palmo, T.; Beckham, S. A.; Wilce, M. C. J.; Johnson, P. E. Quinine Binding by the Cocaine-Binding Aptamer. Thermodynamic and Hydrodynamic Analysis of High-Affinity Binding of an Off-Target Ligand. *Biochemistry* **2013**, *52* (48), 8652−8662.
(32) Desrosiers, A.; Derbali, R. M.; Hassine, S.; Berdugo, J.; Long, V.; Lauzon, D.; De Guire, V.; Fiset, C.; DesGroseillers, L.; Leblond Chain, J.; et al. Programmable self-regulated molecular buffers for precise sustained drug delivery. *Nat. Commun.* **2022**, *13* (1), 6504.
(33) Zhang, D. Y.; Winfree, E. Control of DNA Strand Displacement Kinetics Using Toehold Exchange. *J. Am. Chem. Soc.* **2009**, *131* (47), 17303−17314.
(34) Simmel, F. C.; Yurke, B.; Singh, H. R. Principles and Applications of Nucleic Acid Strand Displacement Reactions. *Chem. Rev.* **2019**, *119* (10), 6326−6369.
(35) Copeland, R. A. The drug−target residence time model: a 10-year retrospective. *Nat. Rev. Drug Discovery* **2016**, *15* (2), 87−95.
(36) Cusack, K. P.; Wang, Y.; Hoemann, M. Z.; Marjanovic, J.; Heym, R. G.; Vasudevan, A. Design strategies to address kinetics of drug binding and residence time. *Bioorg. Med. Chem. Lett.* **2015**, *25* (10), 2019−2027.
(37) Holderfield, M.; Lee, B. J.; Jiang, J.; Tomlinson, A.; Seamon, K. J.; Mira, A.; Patrucco, E.; Goodhart, G.; Dilly, J.; Gindin, Y.; et al. Concurrent inhibition of oncogenic and wild-type RAS-GTP for cancer therapy. *Nature* **2024**, *629* (8013), 919−926.
(38) Schulze, C. J.; Seamon, K. J.; Zhao, Y.; Yang, Y. C.; Cregg, J.; Kim, D.; Tomlinson, A.; Choy, T. J.; Wang, Z.; Sang, B.; et al. Chemical remodeling of a cellular chaperone to target the active state of mutant KRAS. *Science* **2023**, *381* (6659), 794−799.
(39) Jiang, J.; Jiang, L.; Maldonato, B. J.; Wang, Y.; Holderfield, M.; Aronchik, I.; Winters, I. P.; Salman, Z.; Blaj, C.; Menard, M.; et al. Translational and Therapeutic Evaluation of RAS-GTP Inhibition by RMC-6236 in RAS-Driven Cancers. *Cancer Discovery* **2024**, *14* (6), 994−1017.
(40) Li, C.; Vides, A.; Kim, D.; Xue, J. Y.; Zhao, Y.; Lito, P. The G protein signaling regulator RGS3 enhances the GTPase activity of KRAS. *Science* **2021**, *374* (6564), 197−201.
(41) Uhrich, K. E.; Cannizzaro, S. M.; Langer, R. S.; Shakesheff, K. M. Polymeric Systems for Controlled Drug Release. *Chem. Rev.* **1999**, *99* (11), 3181−3198.
(42) Brayden, D. J. Controlled release technologies for drug delivery. *Drug Discovery Today* **2003**, *8* (21), 976−978.
(43) Janin, J.; Chothia, C. The structure of protein-protein recognition sites. *J. Biol. Chem.* **1990**, *265* (27), 16027−16030.
(44) Ke, W.; Laurent, A. H.; Armstrong, M. D.; Chen, Y.; Smith, W. E.; Liang, J.; Wright, C. M.; Ostermeier, M.; van den Akker, F. Structure of an Engineered β-Lactamase Maltose Binding Protein Fusion Protein: Insights into Heterotropic Allosteric Regulation. *PLoS One* **2012**, *7* (6), No. e39168.
(45) Munzar, J. D.; Ng, A.; Corrado, M.; Juncker, D. Complementary oligonucleotides regulate induced fit ligand binding in duplexed aptamers. *Chem. Sci.* **2017**, *8* (3), 2251−2256.
(46) Munzar, J. D.; Ng, A.; Juncker, D. Comprehensive profiling of the ligand binding landscapes of duplexed aptamer families reveals widespread induced fit. *Nat. Commun.* **2018**, *9* (1), 343.

https://doi.org/10.1021/jacs.4c08597
J. Am. Chem. Soc. XXXX, XXX, XXX−XXX